

Recent developments in high energy physics

S N GANGULI

Tata Institute of Fundamental Research, Homi Bhabha Road, Mumbai 400 005, India

Abstract. Recent results from experiments with solar, atmospheric and accelerator neutrinos are presented. Some of the important results from the LEP and TEVATRON colliders are summarised.

Keywords. Neutrino oscillations; solar neutrinos; atmospheric neutrinos; Standard Model; Higgs and SUSY.

1. Introduction

This symposium covered various topics in the field of high energy physics and they may be classified into six classes: (i) string theory, (ii) neutrino oscillations, (iii) Standard Model and beyond, (iv) heavy ion physics, (v) high energy astrophysics and (vi) experiments at large hadron collider (LHC). There were 21 plenary talks and about 100 contributed papers presented in the symposium. This review is expected to bring out the perspectives and highlights of the symposium.

2. Neutrino oscillations

Experiments with neutrinos started some forty years ago and these studies have led to some remarkable results. Neutrinos were instrumental in confirming V-A theory of weak interactions and provided the first evidence of gravitational collapse from the supernova SN1987A; the discovery of neutral current interactions, the measurement of electroweak mixing angle $\sin^2 \theta_W$ and detailed measurements of nuclear structure functions etc. are some of the vital results from neutrino experiments. However one knows only a few intrinsic properties of the neutrinos: neutrinos are left handed, while the antineutrinos are right handed; neutrinos carry a lepton flavour quantum number and there are only three light neutrinos (ν_e, ν_μ and ν_τ) with standard couplings as observed from Z decays at LEP. However one does not know whether neutrinos have a mass. There have been several attempts to measure neutrino mass directly from decay processes involving neutrinos, but they all resulted in giving upper limits to neutrino mass (a few eV to ν_e from β -decay of tritium, about 170 keV to ν_μ from $\pi^+ \rightarrow \mu^+ + \nu_\mu$, and about 20 MeV to ν_τ from τ decay).

If the neutrinos have a mass, one general possibility is that a neutrino of a given flavour is a coherent superposition of mass eigenstates leading to neutrino oscillation [1]. Oscillations are basically spontaneous conversions between neutrinos of different flavours governed by mixing angle.

See-saw mechanism: As discussed in the following sections, the neutrinos do seem to have mass, but much lighter than the charged leptons and quarks. Unlike charged particles, neutrinos could be of Majorana type or Dirac type. A neutrino which is its own antiparticle is called a Majorana neutrino and has two states: one with spin up and the other with spin down (in this case $\bar{\nu}$ is no different from ν except for its right handed helicity). A neutrino which is distinct from its antiparticle is called a Dirac neutrino and has four states: two states of spin up and spin down for each of ν and $\bar{\nu}$. The explanation why the neutrinos are so much lighter than the charged leptons and quarks is given by the see-saw mechanism [2], which is briefly summarised as follows.

In a field theory description of ν , one can split a Dirac neutrino D into two non-degenerate Majorana neutrinos: ν and N . The following mass relation exists between them: $M_\nu M_N \approx M_D^2$. It is reasonable to assume that the mass M_D of the Dirac particle D is of the same order as the typical mass of the charged lepton, M_l . With this one gets: $M_\nu \sim M_l^2/M_N$. If we suppose that the neutrino N is very heavy, i.e. $M_N \gg M_l$, then we get $M_\nu \ll M_l$. This is the ‘see-saw mechanism’ which yields one very light neutrino and the other a very heavy neutrino reflecting probably a high mass scale of some new physics. It may be noted that in this mechanism the neutrinos are Majorana particles.

Simplified scenario of two neutrino flavour mixing (vacuum oscillation): In this scenario the neutrino oscillation probability, P , is defined as the probability of observing, as an example, a ν_e at a distance L from the source, given that a ν_μ was produced at the source at $L = 0$:

$$P(\nu_\mu \rightarrow \nu_e) = \sin^2 2\theta \cdot \sin^2 \left(\frac{1.27 \cdot \Delta m^2 \cdot L}{E_\nu} \right) \quad (1)$$

$$\equiv \sin^2 2\theta \cdot \sin^2 \left(\frac{\pi L}{\lambda} \right), \quad (2)$$

where $\lambda = \pi E_\nu / 1.27 \cdot \Delta m^2$ as the oscillation length, $A = \sin^2 2\theta$ as the amplitude of oscillation, θ as the mixing angle, $\Delta m^2 = |m_2^2 - m_1^2|$ in eV^2 , E_ν in GeV , and L , which is the distance of the detector from the ν source, is in km . Basically there are two variables: Δm^2 and $\sin 2\theta$.

The following observations are in order: (i) the ideal distance of the detector from the source for observing oscillation is $L = \lambda/2$, so that $\sin^2(\pi L/\lambda) = 1$; (ii) for small values of Δm^2 one needs large values of (L/E) to see oscillations; (iii) for $L < \lambda/4$ the oscillation effect is negligible; (iv) for $L > n\lambda$, with $n \gg 1$, the oscillation effect will get washed out due to spread in E_ν ; (v) if the amplitude of oscillation $\sin^2 2\theta$ is small, one needs large statistics to see oscillation; (vi) in an experiment if P_{exp} is the upper limit, say at 90% CL, of the probability of oscillation, one then obtains $(\Delta m^2)_{\text{min}} = \frac{E}{1.27L} \cdot \sqrt{P_{\text{exp}}}$, and $\sin^2(2\theta_{\text{min}}) \simeq 2P_{\text{exp}}$; and (vii) as is clear from eq. (1), Δm^2 is dependent on (E/L) . The table 1 below shows the expected values of Δm^2 from different neutrino sources.

Three neutrino flavour mixing: In this scenario one dominant mass scale has been assumed, where two neutrinos (ν_e and ν_μ) are supposed to have negligible mass with very very small

Table 1. Expected Δm^2 from neutrino sources.

Neutrino source	E	L	Δm^2 (eV ²)
Solar	1–10 MeV	10^{11} m	10^{-10} – 10^{-11}
Atmospheric	1–10 GeV	10 – 10^4 km	1 – 10^{-4}
Accelerator	1–50 GeV	~ 1 km	≥ 1
	1–50 GeV	$\sim 10^3$ km	10^{-3}
Reactor	3 MeV	1 km	10^{-3}

mass difference (basically to account for solar neutrino deficit) and the third neutrino (ν_τ) to have larger mass compared to the first two (to account for atmospheric neutrino observations). There are three variables in this scenario: one mass difference and two mixing angles.

MSW effect [3]: In this scenario the neutrino oscillation is enhanced by the dense medium through which neutrinos travel. This can be rephrased as if neutrinos undergo a change due to refractive index while passing through dense medium and this depends dominantly on neutral current amplitude (for ν_e, ν_μ and ν_τ), charged current amplitude (for ν_e), density of electrons in the medium and momentum of neutrinos. For the range of solar densities the enhancement is expected for oscillation length in the range: $\lambda \simeq 10^4$ to 10^8 m, which corresponds to Δm^2 in the range 10^{-4} to 10^{-9} eV².

Neutrino sources and types of experiments: There are three different neutrino sources which are used for experiments: (i) solar neutrinos, (ii) atmospheric neutrinos and (iii) neutrinos from accelerators and reactors. Neutrino experiments are divided into two categories: (a) *Disappearance experiments*: In this type of experiments one measures the flux of a given neutrino flavour at a certain distance L from the source (the flux is known at $L = 0$), i.e., one measures the probability $P(\nu_i \rightarrow \nu_i)$, where $i = e, \mu, \tau$; the probability smaller than one will signify the conversion of neutrino to another flavour. (b) *Appearance experiments*: In these experiments one uses beams of one neutrino flavour and search for neutrinos of different flavour at a certain distance L from the source, i.e., one measures the probability $P(\nu_i \rightarrow \nu_j)$, where $i \neq j$. Measurements are also made as a function of E , L/E and θ , where L = distance between the neutrino source and the detector, E is the energy of the neutrinos and θ is the zenith angle.

2.1 Solar neutrinos

Solar neutrinos, ν_e , are produced via nuclear reactions in the sun, and these reactions are listed in the table 2 below.

Basically there are four nuclear reactions which are responsible for neutrino source: pp , pep , ${}^7\text{Be}$ and ${}^8\text{B}$. We have not shown contribution of ‘ hep ’ reaction and CNO cycle as they are negligible. There are four experiments taking data for solar neutrinos and these are briefly described below.

(a) *Homestake* [4]: The chlorine detector in Homestake mine is taking data since last thirty

Table 2. Neutrino producing reactions in the Sun.

Reaction
$p + p \rightarrow {}^2\text{H} + e^+ + \nu_e + 0.42 \text{ MeV} (99.75\%)$
$p + e^- + p \rightarrow {}^2\text{H} + \nu_e + 1.44 \text{ MeV} (0.25\%)$
${}^2\text{H} + p \rightarrow {}^3\text{He} + \gamma + 5.49 \text{ MeV}$
${}^3\text{He} + {}^3\text{He} \rightarrow \alpha + 2p + 12.86 \text{ MeV} (86\%)$
${}^3\text{He} + \alpha \rightarrow {}^7\text{Be} + \gamma + 1.59 \text{ MeV} (14\%)$
${}^7\text{Be} + e^- \rightarrow {}^7\text{Li} + \nu_e + 0.86 \text{ MeV} (99.89\%)$
${}^7\text{Be} + p \rightarrow {}^8\text{B} + \gamma + 0.14 \text{ MeV} (0.11\%)$
${}^8\text{B} \rightarrow {}^8\text{Be} + e^+ + \nu_e + 14.6 \text{ MeV}$

Table 3. Details of solar neutrino experiments; bracketed numbers indicate predicted fraction of neutrino source.

Experiment	Neutrino source	Reaction
Homestake	${}^7\text{Be}(0.15), {}^8\text{B}(0.78)$	$\nu_e + {}^{37}\text{Cl} \rightarrow {}^{37}\text{Ar} + e^-$
SAGE and GALLEX	$pp(0.54), {}^7\text{Be}(0.27)$ ${}^8\text{B}(0.10)$	$\nu_e + {}^{71}\text{Ga} \rightarrow {}^{71}\text{Ge} + e^-$
Kamiokande and SK	${}^8\text{B}(1.0)$	$\nu + e^- \rightarrow \nu + e^-$

years. It contains 520 tons of chlorine. This is the first experiment to detect solar neutrinos and it is sensitive to solar neutrinos from ${}^7\text{Be}$ and ${}^8\text{B}$, with detection threshold energy of neutrino as 0.8 MeV. Its observation of only 33% of neutrino flux compared to the prediction of standard solar model (SSM) led to the ‘solar neutrino puzzle’.

(b) *Gallex and SAGE* [5,6]: The two detectors GALLEX and SAGE are using gallium (30 tons and 60 tons respectively) as the sensitive target for the experiment. Experiments are sensitive to solar neutrinos from pp , ${}^7\text{Be}$ and ${}^8\text{B}$ (with detection threshold energy of neutrino as 0.2 MeV). The GALLEX and SAGE detectors have been calibrated in the laboratory by intense neutrino source from ${}^{51}\text{Cr}$. These two experiments observe $\sim 50\%$ of neutrino flux compared to the prediction of SSM.

(c) *Super-Kamiokande (SuperK)* [7]: Super-Kamiokande (SuperK) is an upgraded version of Kamiokande in Kamioka mine in Japan. It uses 50000 tons of water as water Cherenkov detector with 12000 photomultipliers. The detector is sensitive to solar neutrinos from ${}^8\text{B}$, with detection threshold energy of neutrino as 7.0 MeV. This detector is direction sensitive and gave the first real proof that neutrinos come from the sun from the scattering of ν_e with electrons. Because of its real time capabilities it could measure day/night effects in neutrino flux. This experiment observes $\sim 50\%$ of neutrino flux compared to the prediction of SSM.

Table 3 summarises some of the details of these experiments.

Table 4. Experimental results from solar neutrino.

Experiment	Data	Theory	Data/Theory
Homestake ^(a)	$2.56 \pm 0.16 \pm 0.14$	$7.7^{+1.2}_{-1.0}$	0.33 ± 0.06
SAGE ^(a)	$66.6^{+7.8}_{-8.1}$	129^{+8}_{-6}	0.52 ± 0.07
GALLEX ^(a)	$77.5 \pm 6.2 \pm 4.5$	129^{+8}_{-6}	0.60 ± 0.07
Kamiokande ^(b)	$2.80 \pm 0.19 \pm 0.33$	$5.15^{+1.0}_{-0.7}$	0.54 ± 0.11
Super-Kamiokande ^(b)	$2.44 \pm 0.05 \pm 0.08$	$5.15^{+1.0}_{-0.7}$	0.47 ± 0.08

^(a)Rate is in unit of SNU; 1 SNU = 10^{-36} captures per target atom per second.

^(b)In unit of 10^6 neutrinos \cdot cm $^{-2}$ \cdot s $^{-1}$.

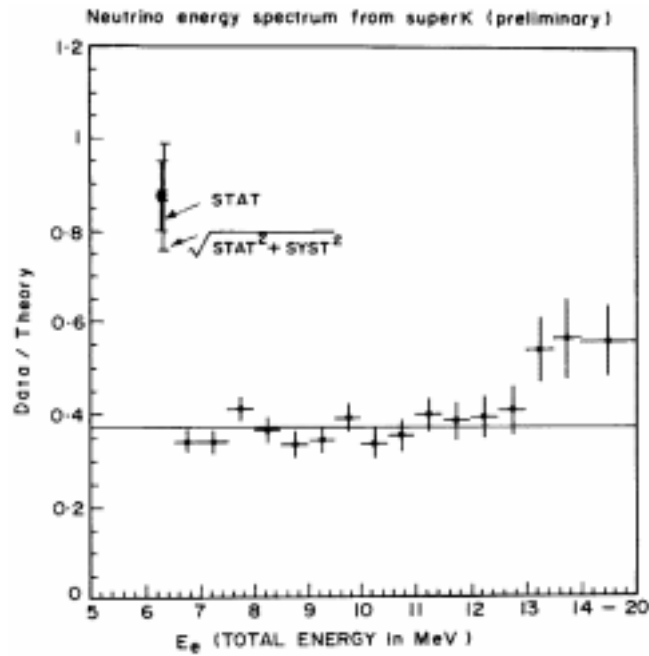


Figure 1. Neutrino energy spectrum from the Sun. The plot shows recoil electron energy in MeV. The fit to the flat shape for no oscillation hypothesis yields $\chi^2 = 25/15$.

Experimental results from these experiments are summarised in table 4.

From the above experimental data there is a clear evidence for a deficit of solar neutrino by $\geq 3.5\sigma$ with respect to expectation from the standard solar model (SSM) [8].

ν energy spectrum from super-Kamiokande: The super-K has also measured the ν energy spectrum from the Sun. In the figure 1 is shown the data/theory as a function of ν energy. The following conclusions are drawn from the measurement: (a) there is a deficit of data throughout from 7 MeV to 20 MeV with respect to the expectation from SSM, (b) the shape

of the data is the same up to ≤ 13 MeV with a constant factor of 0.368 for data/theory. Beyond 14 MeV there is an excess indicating energy dependence in shape with respect to SSM.

Global analysis: Several analyses have been carried out by Hata and Langacker [9], Bahcall *et al* [10], Fogli *et al* [11] and Narayan *et al* [12].

We present here the results of Bahcall *et al*. The following input data is used: (i) Total ν flux measurements of Homestake, Gallex, Sage and super-Kamioka; (ii) energy dependence of the flux from super-Kamioka and (iii) variation in flux of day/night.

Results of the global analysis are as follows:

(a) *MSW scenario and two ν mixing hypothesis:* Best fit to the small mixing angle hypothesis yields (confidence level (CL) of fit is 7%) $\Delta m^2 = 5 \times 10^{-6} \text{eV}^2$; $\sin^2 2\theta = 5.5 \times 10^{-3}$.

(b) *Vacuum oscillation with two ν mixing hypothesis:* Best fit to the data yields (CL of fit is 6%) $\Delta m^2 = 6.5 \times 10^{-11} \text{eV}^2$; $\sin^2 2\theta = 0.75$.

(c) *No oscillation hypothesis:* Assuming no oscillation, two results are reported: (i) arbitrary combination of theoretical solar ν fluxes from pp , ${}^7\text{Be}$, ${}^8\text{B}$ and CNO lead to inconsistency with data at 3.5σ level, (ii) direct fit with the standard solar model leads to inconsistency with the data at 20σ level.

2.2 Atmospheric neutrinos

Atmospheric neutrinos are produced by interactions of high energy cosmic ray particles (protons, alpha etc.) with air nuclei leading to production of pions, kaons etc which subsequently decay yielding ν_e and ν_μ . As a result of the decay e.g.: $\pi^+ \rightarrow \mu^+ \nu_\mu$; and $\mu^+ \rightarrow e^+ \nu_e \bar{\nu}_\mu$, one expects the flux of ν_μ to be twice that of ν_e , i.e., $(\nu_\mu + \bar{\nu}_\mu)/(\nu_e + \bar{\nu}_e) \simeq 2$. However, with the increasing energy this ratio becomes larger than 2, because the first generation ν_μ from π decay is of much larger energy than the ν from decay of second generation μ .

It may be noted that atmospheric neutrinos are much less abundant than the solar neutrinos. But these are high energy neutrinos in the range ~ 100 MeV to ~ 100 GeV (in comparison solar neutrino energies are in the range ~ 1 to 15 MeV) and are easily detected via the following charged current reactions: $\nu_\mu + N \rightarrow \mu + X$, and $\nu_e + N \rightarrow e + X$.

Besides measuring the ratio ν_μ/ν_e , one also measures the zenith angle dependence of the flux ratio $\nu_{\text{up}}/\nu_{\text{down}}$. Since the detector is on the surface of the earth, the path length available for neutrinos coming from up is only ~ 10 km, while the neutrinos coming from down will have to cross the earth diameter which is ~ 10000 km or more. If there is no oscillation one expects $\nu_{\text{up}}/\nu_{\text{down}} \simeq 1$ for $E_\nu \geq 1$ GeV.

Experimental results

I. *Measurement of $R = [(\nu_\mu/\nu_e)_{\text{Data}}/(\nu_\mu/\nu_e)_{\text{MC}}]$:* Experimentally one measures the ratio ν_μ/ν_e by detecting muons and electrons via charged current reactions. In order to remove the uncertainties in the systematics of neutrino flux calculation, interaction cross section and fiducial volume of the detector used for the detection of muons and electrons, one

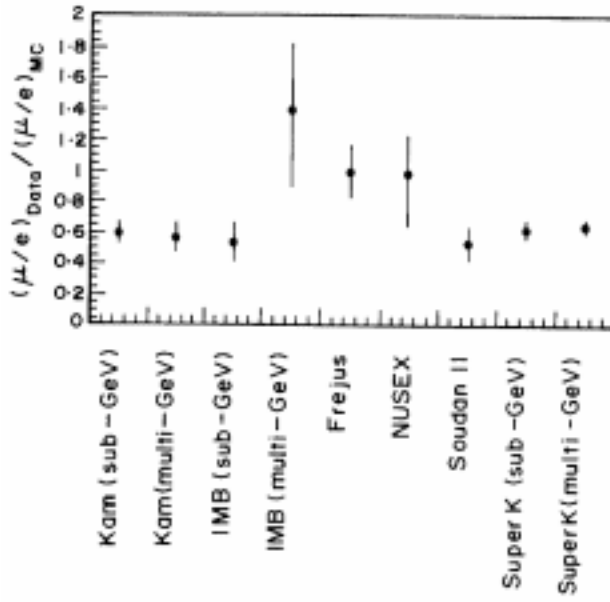


Figure 2. The plot summarises the values of $R = (\nu_\mu/\nu_e)_{\text{Data}}/(\nu_\mu/\nu_e)_{\text{MC}}$ as measured by different experiments.

determines the ratio of ratios, R , which is given by: $R = (\nu_\mu/\nu_e)_{\text{Data}}/(\nu_\mu/\nu_e)_{\text{MC}}$. The quantity $(\nu_\mu/\nu_e)_{\text{MC}}$ refers to the Monte Carlo prediction of the flux ν_μ/ν_e . The expected value of R is unity. The values of R as measured by different experiments are summarised in figure 2.

The most precise measurements are from super-Kamiokande and these are:

$$R_{\text{S-K}}^{\text{sub-GeV}} = 0.626 \pm 0.026 \pm 0.010 \pm 0.049, \quad (3)$$

$$R_{\text{S-K}}^{\text{multi-GeV}} = 0.654 \pm 0.051 \pm 0.019 \pm 0.078. \quad (4)$$

It is clear that the value of R is much less than unity.

II. Zenith angle distributions from super-Kamiokande: The zenith angle distributions of electron-like events (produced by ν_e) and muon-like events (produced by ν_μ) as a function of $\cos \theta$ are shown in figure 3. It is to be noted that (a) $\cos \theta = -1$ to -0.2 is for upward going ν while $\cos \theta = +1$ to $+0.2$ refers to downward going neutrinos. In the multi-GeV category super-Kamiokande has observed a total of 290 events for e -like and 531 events for μ -like. If there is no oscillation one expects $(U - D)/(U + D) = 0$, where U refers to upward going while D for downward going neutrinos for the values of $\cos \theta$ as defined above. The hatched blocks in the figure refer to MC prediction with no oscillation. Results from super-Kamiokande are summarised below:

$$\left(\frac{U - D}{U + D} \right)_{e\text{-like}} = -0.036 \pm 0.067 \pm 0.02$$

$$\Rightarrow \text{consistent with zero, i.e. no oscillation}, \quad (5)$$

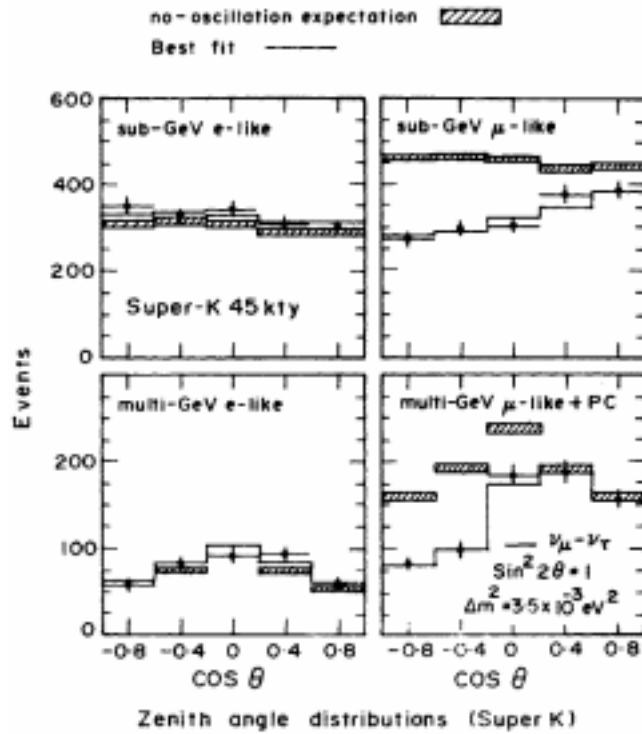


Figure 3. Zenith angle distributions from super-K for e -like and μ -like events.

$$\left(\frac{U-D}{U+D}\right)_{\mu\text{-like}} = -0.296 \pm 0.048 \pm 0.01$$

$$\Rightarrow 6\sigma \text{ discrepancy with no oscillation.} \quad (6)$$

The following conclusions are drawn: (i) e -like events are consistent with no oscillation, and (ii) there is a depletion of μ -like events from upward moving neutrinos and it disagrees with no oscillation hypothesis by more than six sigma.

III. *Momentum dependence of up-down asymmetry*: Super-Kamiokande has also given momentum dependence of up-down asymmetry and it is shown in figure 4. The hatched blocks refer to MC prediction with no oscillation. It is seen that e -like events are in agreement with the expectation from Monte Carlo, while μ -like events are in disagreement with MC. The μ -like events have been fitted with the oscillation hypothesis of $\nu_\mu \rightarrow \nu_\tau$ with $\Delta m^2 = 3.5 \times 10^{-3} \text{ eV}^2$ and $\sin^2 2\theta = 1.0$, and this is shown as dotted line in the figure.

IV. *Up going ν_μ interactions in rocks*: The upward going neutrinos will also interact with rocks of the earth. This will lead to upward going muons from interactions of ν_μ . Results from super-Kamiokande and MACRO detectors are presented in figure 5a and b respectively. Predictions from MC with no oscillation are shown as hatched lines, while the dotted curves in the figures show the prediction for an oscillation with $\Delta m^2 = 2.5 \times 10^{-3} \text{ eV}^2$ and $\sin^2 2\theta = 1.0$.

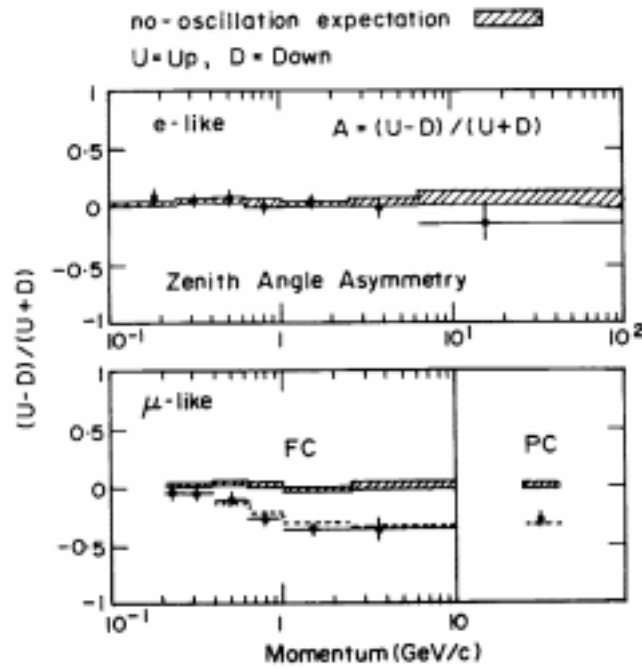


Figure 4. Momentum dependence of up-down asymmetry $A = (U - D)/(U + D)$. Here FC stands for fully contained events and PC for partially contained ones.

V. *Fit to atmospheric data:* Figure 6 shows the allowed regions using zenith angle distributions and double ratio from atmospheric data. Best result is from super-K which yields Δm^2 in the range from 10^{-3} to 10^{-2} eV² and $\sin^2 2\theta$ close to 1.0.

2.3 Accelerator and reactor neutrinos

The LSND experiment: The only experiment to have claimed positive observation of neutrino oscillation ($\nu_\mu \rightarrow \nu_e$) is the LSND (liquid scintillator neutrino detector) experiment at the LAMPF neutrino source [13]. The LAMPF accelerator produces a large number of π^+ from interactions of energetic protons. First part of the LSND experiment consisted in detecting decay of pions at rest (DAR): $\pi^+ \rightarrow \nu_\mu + \mu^+$ followed by muon decays at rest: $\mu^+ \rightarrow e^+ + \nu_e + \bar{\nu}_\mu$. A positive signal was observed for oscillation of $\bar{\nu}_\mu \rightarrow \bar{\nu}_e$ from an excess of $\bar{\nu}_e$ signal via the reaction: $\bar{\nu}_e + p \rightarrow e^+ + n$. The LSND measured oscillation probability is $0.31 \pm 0.09 \pm 0.05\%$. This gets translated into Δm^2 range of 10^{-1} to 10^{+1} eV².

The second part of LSND experiment consisted in studying decay in flight of pions (DIF): $\pi^+ \rightarrow \nu_\mu + \mu^+$. They searched for oscillation of $\nu_\mu \rightarrow \nu_e$ from the appearance of high energy ν_e . The energy of this ν_e should be above the end point of $\mu^+ \rightarrow e^+ + \nu_e + \bar{\nu}_\mu$ decay at rest. The experiment detected a significant excess of ν_e .

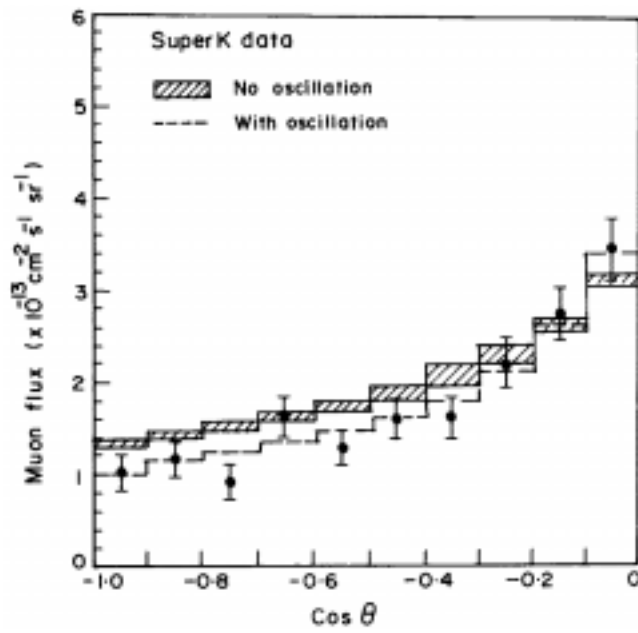


Figure 5a. Zenith angle distribution of up-going muons from ν_μ interactions in rocks from SuperK. Fit to the shape of the distribution with no oscillation hypothesis, shown as hatched histogram, leads to $\chi^2 = 18.3/9$. The dotted histogram shows the prediction with oscillation hypothesis using $\Delta m^2 = 2.5 \times 10^{-3} \text{ eV}^2$ and $\sin^2 2\theta = 1$.

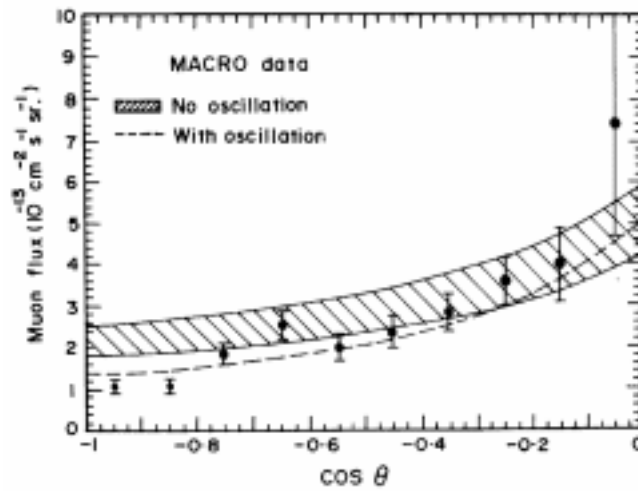


Figure 5b. Zenith angle distribution of up-going muons from MACRO. The solid curve with shaded region shows the expectation from no oscillation hypothesis. The dashed line shows the prediction with oscillation hypothesis using $\Delta m^2 = 2.5 \times 10^{-3} \text{ eV}^2$ and $\sin^2 2\theta = 1$.

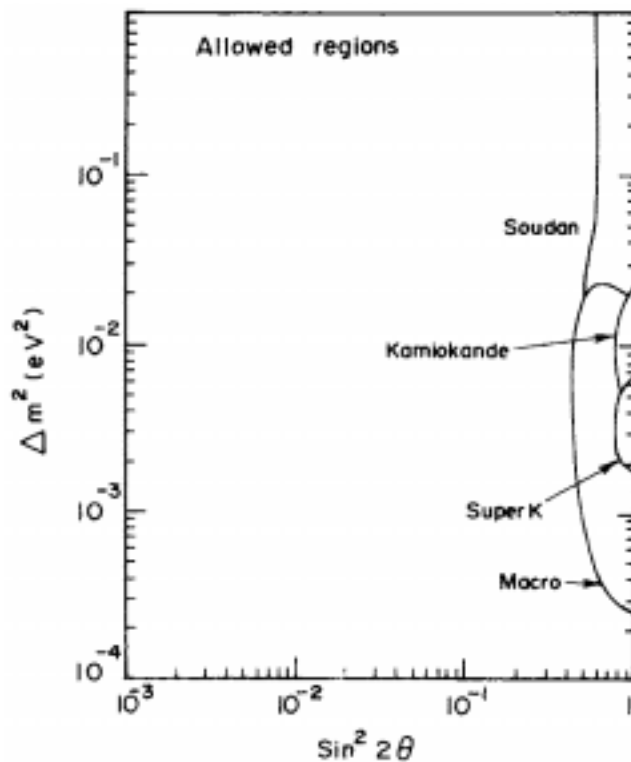


Figure 6. Allowed regions under Δm^2 versus $\sin^2 2\theta$ using zenith angle distributions and double ratio R from the atmospheric data.

Other searches [14]: The KARMEN detector of RAL, with a similar beam and energy range as of LSND, does not see any evidence of oscillation. However, KARMEN currently lacks the sensitivity to rule out convincingly the LSND observation. All searches for $\nu_\mu \leftrightarrow \nu_e$ are summarised in figure 7; this includes results from reactor experiments Chooz and Bugey. Mini-Boone experiment at FNAL is approved and it will be able to cover completely the range of LSND.

The search for $\nu_\mu \rightarrow \nu_\tau$ is being carried out by two dedicated experiments NOMAD and CHORUS at CERN with ν_μ beam of $\langle E_\nu \rangle \sim 15$ GeV and $L \sim 1$ km (these experiments have completed the data taking); their aim is to detect tau lepton from charged current interaction of ν_τ . Their results are summarised in the exclusion plot of figure 8 along with other indirect results.

2.4 Summary of the hints in oscillation

There are two pieces of positive information in neutrino oscillation from solar and atmospheric neutrinos. There is a third piece of positive effect from accelerator based LSND experiment but it needs confirmation from another independent experiment. These results are summarised in table 5.

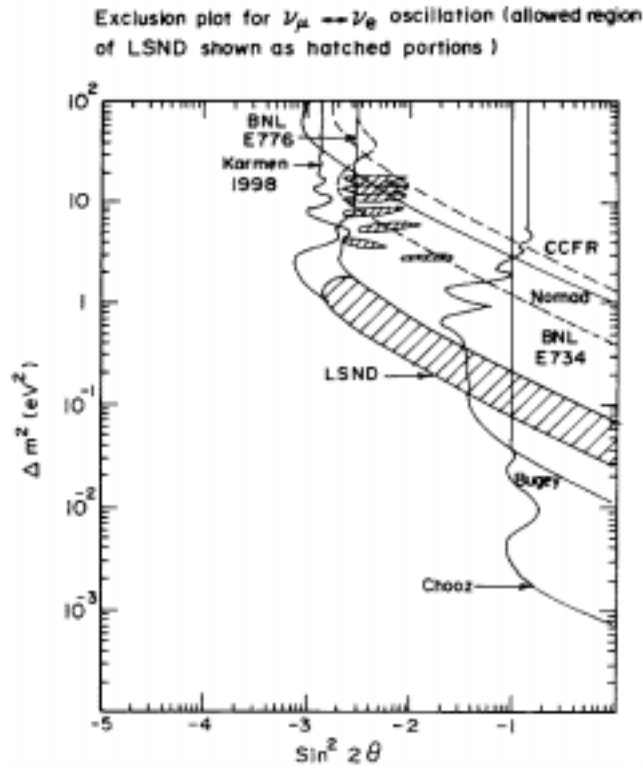


Figure 7. $\nu_\mu \leftrightarrow \nu_e$ oscillation status is shown as exclusion plot; allowed regions of LSND (99% CL) are shown as hatched portions.

Table 5: Positive hints from neutrino oscillations.

ν -source	Oscillation type	Δm^2 (eV ²)	$\sin^2 2\theta$
Solar	$\nu_e \rightarrow \nu_X$	$\leq 10^{-10}$ (vacuum) $\approx 10^{-5}$ (MSW)	~ 1 10^{-3} or 1 (MSW)
Atmospheric	$\nu_\mu \rightarrow \nu_\tau$	10^{-3} to 10^{-2}	≈ 1
LSND	$\nu_\mu \rightarrow \nu_e$	10^{-1} to 10^{+1}	$2 \cdot 10^{-3}$ to $5 \cdot 10^{-2}$

2.5 Future projects

Solar neutrino: Several new experiments are planned. (i) SNO – Canada: This has just started taking data and is a unique detector aiming to detect simultaneously neutral and charged current interactions. This will allow to get total neutrino flux of all flavours

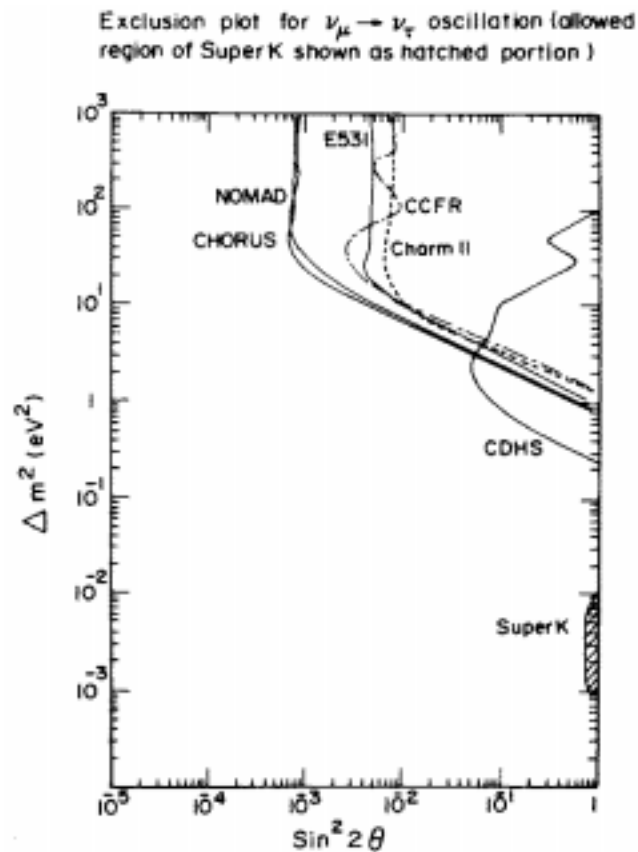


Figure 8. $\nu_\mu \rightarrow \nu_\tau$ oscillation status is shown as exclusion plot; allowed region of SuperK is shown as hatched portion.

from ^8B neutrinos of sun. It has inner detector consisting of 1000 tons of heavy water and outer shell of 7000 tons of water. (ii) Borexino – Gran Sasso: It will use liquid scintillator to detect neutrino electron scattering. It will be able to separate ^7Be neutrinos from others. (iii) There are also several other projects which are planned. *Atmospheric neutrinos*: Super-K, Soudan II and Macro are continuing their data taking. The ICARUS is expected to be operational in 2000 with its liquid argon TPC. *Accelerator neutrinos*: Several long base line experiments are planned. Some of them are summarised in the table 6.

3. Standard model and MSSM

We present here some of the recent results from LEP and TEVATRON, which were discussed in detail during the plenary talks. The main motivation was how to understand the electroweak symmetry breaking mechanism. The simplest mechanism is one

Table 6. Long base line experiments.

Experiment	$\langle E_\nu \rangle$ (GeV)	L (km)	Δm^2 (eV ²) expected
K2K	~ 1 GeV	250	$\sim 2 \cdot 10^{-3}$
MINOS	~ 10 GeV	730	$\sim 10^{-3}$
CERN-NGS	~ 20 GeV	740	$\sim 10^{-3}$

Higgs doublet of the Standard Model leading to one physical Higgs scalar. But this does leave several questions unanswered, e.g. the hierarchy problem. This led to the minimal supersymmetric extension of the Standard Model (MSSM) with two Higgs doublet leading to five physical Higgs particles: h^0, H^0, A^0, H^+ and H^- . The lightest Higgs particle, h^0 , is predicted to be ≤ 150 GeV. There is an indication from the measurements of strong, electromagnetic and weak couplings that with the supersymmetry there is a grand unification of the three forces at $\sim 10^{16}$ GeV. Theoretical details of supersymmetry phenomenology and related topics were covered in the symposium by several theory talks and will not be discussed here. Here we confine ourselves to experimental measurements.

3.1 Measurements of W boson properties

W boson mass is being measured at LEP2 [15] since 1996 with center of mass energies (\sqrt{s}) of 161, 172, 183, 189, 192, 196 and 200 GeV. W bosons at LEP are produced in pairs: $e^+e^- \rightarrow W^+W^-$, followed by decays of $W : W^+W^- \rightarrow l^+\nu l^-\bar{\nu}, l\nu q\bar{q}', q\bar{q}'q\bar{q}'$, where l and q stand for lepton and quark respectively. Results are available from runs at 161, 172, 183 and 189 GeV. Results from recent runs at 192, 196 and 200 GeV are awaited. W mass measurements from $W^+W^- \rightarrow q\bar{q}'q\bar{q}'$ may be affected by the colour reconnection as the W decay length, which is ~ 0.1 fm, is much smaller than the hadronization scale of ~ 1 fm. Within errors, the two experimental measurements of W mass: $M_W(l\nu q\bar{q}') = 80.31 \pm 0.11$ GeV and $M_W(q\bar{q}'q\bar{q}') = 80.39 \pm 0.14$ GeV, are found to be in agreement and hence the average of the two values is used for the W mass. W mass results from LEP2 and from TEVATRON (CDF and DZERO) [16] are summarised below:

$$M_W(\text{LEP2}) = 80.37 \pm 0.09 \text{ GeV}, \quad (7)$$

$$M_W(\text{TEVATRON}) = 80.41 \pm 0.09 \text{ GeV}, \quad (8)$$

$$\text{Average } M_W = 80.39 \pm 0.06 \text{ GeV}. \quad (9)$$

The above average value of 80.39 ± 0.06 GeV may be compared with the indirect estimate from LEP1/SLD value of 80.332 ± 0.037 GeV.

The W width has been measured at Tevatron and LEP with an uncertain of ~ 200 MeV and is in agreement with the expectation from Standard Model width of 2.07 GeV.

W branching ratios as measured at LEP2 are in good agreement with the expectations of the Standard Model: $\text{Br}(W \rightarrow l\nu) = 10.8\%$ and $\text{Br}(W \rightarrow \text{hadrons}) = 67.5\%$.

3.2 Top quark

The top quark mass has been measured at the 1.8 TeV $\bar{p}p$ collider at Tevatron. Top quarks are produced dominantly in pairs via the reactions: $q + \bar{q} \rightarrow t + \bar{t}$ and $g + \bar{g} \rightarrow t + \bar{t}$, where g stands for a gluon. Top quark decay is dominated by two body mode: $t \rightarrow W + b$ where b stands for a b quark. Final states from $t\bar{t}$ decay are classified into three categories: ‘all jets’, ‘single lepton + jets’ and ‘dilepton + jets’. Results from Tevatron [17] are summarised below:

$$M_{\text{top}}(\text{CDF}) = 175.3 \pm 4.1 \pm 5.0 \text{ GeV}, \quad (10)$$

$$M_{\text{top}}(\text{DZERO}) = 172.1 \pm 5.2 \pm 4.9 \text{ GeV}, \quad (11)$$

$$\text{Average } M_{\text{top}} = 173.8 \pm 5.0 \text{ GeV}. \quad (12)$$

The values of the production cross-section of top quark are: $7.6^{+1.8}_{-1.5}$ pb (CDF); $5.9 \pm 1.1 \pm 1.2$ pb (DZERO), and within errors these are in agreement with the expectation.

3.3 Higgs searches at LEP

Direct searches of scalar Higgs at LEP have provided only a lower limit and it is: $M_{\text{Higgs}} > 95$ GeV at 95% CL.

Indirect estimate on Higgs mass has been carried out by fitting all the existing electroweak measurements at LEP, SLD and $\bar{p}p$ collider along with the measurement of electroweak mixing angle from νN interactions and it yielded the mass of Higgs [15] as 76^{+85}_{-47} GeV, with an upper limit of 262 GeV at 95% CL; a plot showing $\Delta\chi^2$ versus m_H is shown in figure 9.

3.4 Search for supersymmetry (SUSY) particles

In the minimal extension of the standard model (MSSM) every known particle has a SUSY partner differing in spin by a half unit: l (lepton) $\rightarrow \tilde{l}$ (slepton), q (quark) $\rightarrow \tilde{q}$ (squark), gluon \rightarrow gluino, photon \rightarrow photino, gauge bosons and Higgs \rightarrow charginos ($\tilde{\chi}^\pm$) and neutralinos ($\tilde{\chi}^0$) etc. The lightest among the neutralinos is expected to be stable. This opens up a zoo of new particles with masses greater than or about 100 GeV. All the searches made so far proved to be negative and only lower limits have been provided by various experiments. Some of the lower limits are: (i) ~ 80 GeV for sleptons, (ii) ~ 85 GeV for squarks, (iii) ~ 90 GeV for charginos and (iv) 30 GeV for neutralino.

3.5 CP violation from B decays

CP violation has been observed in the neutral K decays [18]: $K_L^0 \rightarrow \pi^+\pi^-$ and $K_L^0 \rightarrow \pi l \nu$. In the Standard Model with three generations, the quark mass eigenstates are not the same as the weak eigenstates and the matrix relating these bases is described by the

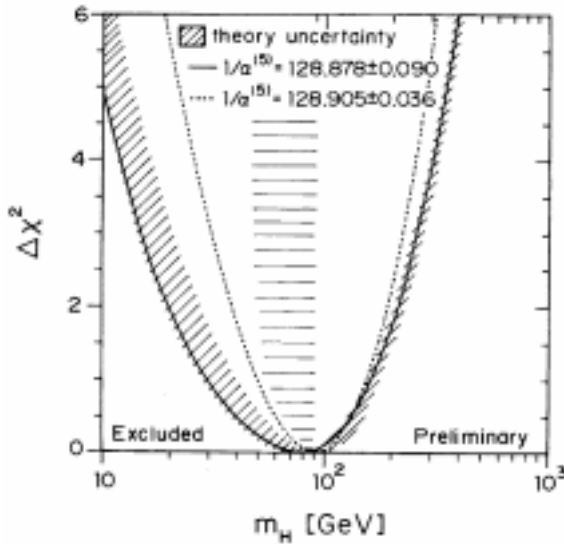


Figure 9. $\Delta\chi^2 = \chi^2 - \chi_{\min}^2$ vs. m_H curve from the result of the fit using all electroweak data including direct measurements of m_W and m_{top} . The hatched band around the solid curve represents an estimate of the theoretical error. The vertical band shows the 95% CL exclusion limit on m_H from the direct search.

Cabbibo–Kobayashi–Maskawa (CKM) mixing matrix and the parametrization of the mixing matrix may be made in terms of three angles and one phase. CP violation arises as a result of the single phase in CKM mixing matrix, and it solely arises due to nonzero value of this phase. The unitarity condition of the CKM matrix can be represented as triangles in the complex plane: α, β and γ .

The decays of neutral B mesons into CP eigenstates (f_{CP}) can allow clean theoretical interpretation in terms of the parameters of the Standard Model. For the B decay f_{CP} could be $J/\psi K_S$ or $\pi\pi$. If CP is violated then the partial decay rates of B and \bar{B} will not be the same, i.e., $\Gamma(B \rightarrow f_{\text{CP}}) \neq \Gamma(\bar{B} \rightarrow f_{\text{CP}})$.

The CDF collaboration [19] at the $\bar{p}p$ collider of Tevatron measured the time dependence of the asymmetry from $B_d^0/\bar{B}_d^0 \rightarrow J/\psi K_s^0$. The asymmetry is given by

$$A_{\text{CP}}(t) = \frac{\bar{B}_d^0(t) - B_d^0(t)}{\bar{B}_d^0(t) + B_d^0(t)} \quad (13)$$

$$= \sin(2\beta) \cdot \sin(\Delta m_d \cdot t). \quad (14)$$

The CDF collaboration from a total of 198 ± 17 events of B_d^0/\bar{B}_d^0 identified by a special tagging method measured the value of $\sin(2\beta)$ which is different from zero. The angle β has also been measured earlier by OPAL collaboration at LEP but with a large uncertainty. The CDF value is given below:

$$\sin(2\beta) = 0.79_{-0.44}^{+0.41} \quad (15)$$

This measurement is the direct indication of the violation of CP symmetry in the b quark system and is consistent with the Standard Model expectation of a large positive value of $\sin(2\beta)$ as 0.75 ± 0.09 [20].

4. Future outlook

There are four key issues which need to be pursued and will be studied during the next decade or so and these are: (i) neutrino mass from neutrino oscillations, (ii) CP violation in the b sector, (iii) search for Higgs and SUSY particles and (iv) search for the onset of quark gluon plasma (QGP).

Several new experiments for solar neutrinos are planned, e.g. the Soudan neutrino observatory (SNO) using deuterium as the target to measure the total integrated flux of all ^8B neutrinos that reach the earth, and the Borexino experiment at Gran Sasso with liquid scintillator will be able to isolate the ^7Be neutrino flux from the sun. In the atmospheric neutrino sector, several long base line experiments are planned to cover completely the region explored by super-K and these experiments are: K2K, MINOS and CERN-NGS. Similarly experiments are planned to make checks on the LSND results with MiniBoone, KARMEN-3 etc.

Experiments planned to study CP violation in the b sector are: (i) the SLAC e^+e^- B factory, an asymmetric e^+e^- collider operating on the $\Upsilon(4s)$ resonance, (ii) the KEK e^+e^- B factory similar to the SLAC one, (iii) the HERA-B, (iv) CMS, ATLAS and LHCb at the large hadron collider (LHC) at CERN. The LHC is going to be a 14 TeV proton–proton collider with 7 TeV protons colliding on 7 TeV protons and is expected to be commissioned in the year 2005. The two B factories at SLAC and KEK have been commissioned recently and are taking data. The CDF and DZERO detectors at the Fermilab will restart taking data from next year. The B factories are expected to produce 10^7 – 10^8 $b\bar{b}$ pairs per year while at LHC one will have 10^{12} – 10^{13} $b\bar{b}$ pairs per year.

After the currently successful two operating colliders: LEP (e^+e^-) for the Z and W physics and Tevatron ($\bar{p}p$) for the top quark discovery, the next frontline high energy physics programme will be based on the large hadron collider at CERN with two modes of operations: 14 TeV proton–proton collisions and 5.5 TeV/nucleon heavy ion collisions. The Indian experimental groups are participating in two experiments at LHC: CMS with main thrust to look for Higgs and SUSY particles, and ALICE to explore the formation of the QGP.

The past history has taught us that hadron colliders lead invariably to discovery of new physics, whereas e^+e^- colliders yield finer physics details because of its well defined and point-like initial state (e^+e^-). Thus to complement the LHC programme at CERN, there are proposals to construct next e^+e^- machine which will be a linear collider (LC) with a centre of mass energy in the range 250–500 GeV as a first step and to upgrade it later on to 1000 GeV or more. The proposals are from KEK (Japan), SLAC (USA) and DESY (Germany). Some of the objectives of the linear collider will be to carry out precision studies on top quark production, properties of Higgs and SUSY particles hoping that these will be discovered at LHC or positive hints seen at LHC, photon–photon physics, gauge mediated symmetry breaking mechanism etc. If a LC machine is approved within the next 5 years it may be in operation around 2010. It will be an important step to promote basic science to understand the constituents of matter and the underlying forces.

References

- [1] Z Maki, M Nakagawa and S Sakata, *Prog. Theor. Phys.* **28**, 870 (1962)
B Pontecorvo, *Sov. Phys. JETP* **26**, 984 (1968)

- V Gribov and B Pontecorvo, *Phys. Lett.* **B28**, 493 (1969)
S Bilenky and B Pontecorvo, *Phys. Rep.* **C41**, 225 (1978)
A Mann and H Primakoff, *Phys. Rev.* **D15**, 655 (1977)
- [2] M Gell-Mann, P Ramond and R Slansky, in *Supergravity* edited by D Freedman and P van Nieuwenhuizen (1979) p. 315
T Yanagida, in *Proceedings of the workshop on unified theory and baryon number in the universe* edited by O Sawada and A Sugamoto, Tsukuba, KEK (1979)
R Mohapatra, G Senjanovic, *Phys. Rev. Lett.* **44**, 912 (1980); *Phys. Rev.* **D23**, 165 (1981)
- [3] L Wolfenstein, *Phys. Rev.* **D17**, 2369 (1978); *Phys. Rev.* **D20**, 2634 (1979)
S Mikheyev and A Smirnov, *Nuovo. Cimento* **9C**, 17 (1986)
- [4] R Davis, A Mann and L Wolfenstein, *Ann. Rev. Nucl. Part. Sci.* **39**, 467 (1989)
- [5] W Hampel *et al*, *Phys. Lett.* **B388**, 384 (1996)
- [6] J N Abdurashitov *et al*, *Phys. Lett.* **B328**, 234 (1994)
- [7] Y Fukuda *et al*, *Phys. Rev. Lett.* **77**, 1683 (1996); *Phys. Rev. Lett.* **81**, 1562 (1998)
- [8] See for example, J N Bahcall and M H Pinsonneault, *Rev. Mod. Phys.* **60**, 781 (1995)
- [9] N Hata and P Langacker, *Phys. Rev.* **D56**, 6107 (1997)
- [10] J N Bahcall, P I Krastev and A Yu Smirnov, *Phys. Rev.* **D58**, 096016 (1998)
- [11] G L Fogli, E Lisi, A Marrone and G Scioscia, *Phys. Rev.* **D59**, 033001 (1999)
- [12] M Narayan, G Rajasekaran and S Uma Sankar, *Phys. Rev.* **D58**, 031301 (1998)
- [13] LSND Collaboration: C Athanassopoulos *et al*, *Phys. Rev. Lett.* **77**, 3082 (1996)
- [14] See for example, Neutrino Oscillation Workshop, Amsterdam, 1998; Lectures delivered by J Panman during 1999 summer student lecture programme at CERN
- [15] LEP Electroweak Working Group: A combination of preliminary electroweak measurements and constraints on the Standard Model, CERN-EP/99-15, Feb (1999)
- [16] See for example, Y K Kim, in *Proceedings of Lepton-Photon Symposium*, Hamburg (1997)
- [17] See for example, R Partridge, in *Proceedings of International Conference on High Energy Physics*, Vancouver (1998)
- [18] J Christenson *et al*, *Phys. Rev. Lett.* **13**, 138 (1964)
- [19] F Abe *et al*, *Phys. Rev. Lett.* **80**, 2057 (1998); *Phys. Rev.* **D59**, 32001 (1999);
CDF/PUB/BOTTOM/CDF/4855, Feb. (1999)
- [20] S Mele, CERN-EP-98-133, August (1998)